in Proc. 47th Asilomar Conf. Signals, Systems, Computers, Pacific Grove, CA, Nov. 2013

A Distributed Particle-based Belief Propagation Algorithm for Cooperative Simultaneous Localization and Synchronization

Florian Meyer*, Bernhard Etzlinger†, Franz Hlawatsch*, and Andreas Springer†

*Vienna University of Technology, Vienna, Austria, {florian.meyer, franz.hlawatsch}@tuwien.ac.at
†Johannes Kepler University, Linz, Austria, {b.etzlinger, a.springer}@nthfs.jku.at

***Abstract*—We present a factor graph framework and a particle-based belief propagation algorithm for distributed *cooperative simultaneous localization and synchronization* (CoSLAS) in decentralized sensor networks. The proposed algorithm jointly estimates the locations and clock parameters of the network nodes in a fully decentralized fashion. This estimation is based on time measurements and communications only between neighboring nodes, and makes only minimal assumptions about the network topology. A significant reduction of computational complexity can be achieved by a novel particle-based scheme for message multiplication. Simulation results demonstrate the good performance of the proposed CoSLAS algorithm.**

***Index Terms*—Belief propagation, CoSLAS, distributed estimation, factor graph, localization, message passing, network synchronization, particle methods, wireless sensor network.**

I. Introduction

In decentralized wireless sensor networks, cooperative sensor self-localization (CSL) [1] and cooperative synchronization (CS) [2] are often based on timing measurements between neighboring nodes [3]. The resulting strong relation between CSL and CS suggests that synergies may be reaped by performing CSL and CS jointly. However, existing methods for joint CSL-CS [4]–[8] place significant constraints on the network topology. Several state-of-the-art algorithms for pure CSL [1], [9] and pure CS [10], [11] run a message passing scheme on a factor graph [12], which avoids these constrains.

Here, we propose a novel nonparametric—i.e., particle-based—belief propagation (BP) message passing algorithm for *cooperative simultaneous localization and synchronization* (CoSLAS). This algorithm is fully decentralized and makes minimal assumptions about the network topology. It differs from the hybrid parametric/nonparametric BP algorithm for CoSLAS presented in [13] in that it uses a "less detailed" factorization of the posterior probability density function (pdf). Approximations of the likelihood function as in [11] and [13] are avoided and the factor graph has fewer loops. Our algorithm also differs from the original nonparametric BP algorithm [9] (used in [13]) in that it employs a novel scheme for particle-based message multiplication whose complexity scales only linearly with the number of particles. This typically results in a lower complexity, which comes at the cost of higher communication requirements (this drawback can however be avoided by using a parametric message representation for communication [14]).

This paper is organized as follows. The CoSLAS model is described in Section II. The particle-based BP algorithm is developed in Sections III and IV. Finally, simulation results are presented in Section V.

This work was supported by the Austrian Science Fund (FWF) under grant S10603 within the National Research Network SISE, by the Linz Center of Mechatronics (LCM) in the framework of the Austrian COMET-K2 programme, and by the Newcom# Network of Excellence in Wireless Communications of the European Commission.

II. The CoSLAS Model

We consider a set $\mathcal{I} \triangleq \{1,\dots,N\} = \mathcal{M} \cup \mathcal{A}$ of static network nodes, which consists of a subset $\mathcal{M}$ of synchronous master nodes (MNs) with known locations and clocks and a subset $\mathcal{A}$ of asynchronous agent nodes (ANs) with unknown locations and clocks. (Our method can be easily extended to the case where the set of spatial MNs differs from the set of temporal MNs.) An example is shown in Fig. 1. Node $i \in \mathcal{I}$ is located at $\mathbf{x}_i = [x_i \; y_i]^{\mathrm{T}}$, and its local time is

$$c_i(t) = \alpha_i t + \beta_i \,, \tag{1}$$

where α_i and β_i are, respectively, the local clock skew and phase offset with respect to the true time t. The local parameters of node i are thus given by $\boldsymbol{\theta}_i \triangleq [x_i \; y_i \; \alpha_i \; \beta_i]^{\mathrm{T}}$. Two nodes $i,j \in \mathcal{I}$ with $i \in \mathcal{A}$ or $j \in \mathcal{A}$ (or both) are able to communicate if $(i,j) \in \mathcal{C}$ (and, by symmetry, $(j,i) \in \mathcal{C}$), where $\mathcal{C} \subseteq (\mathcal{I}\times\mathcal{I}) \setminus (\mathcal{M}\times\mathcal{M})$. The "neighborhood" $\mathcal{T}_i \subseteq \mathcal{I}\setminus\{i\}$ of agent node $i \in \mathcal{A}$ includes all $j \in \mathcal{I}$ that communicate with i, i.e., $\mathcal{T}_i \triangleq \big\{ j \in \mathcal{I}\setminus\{i\} \,\big|\, (i,j) \in \mathcal{C} \big\}$.

A. Measurement Model

As a basis for estimating their local parameters $\boldsymbol{\theta}_i$ and $\boldsymbol{\theta}_j$, node pairs $(i,j) \in \mathcal{C}$ exchange packets via their wireless link

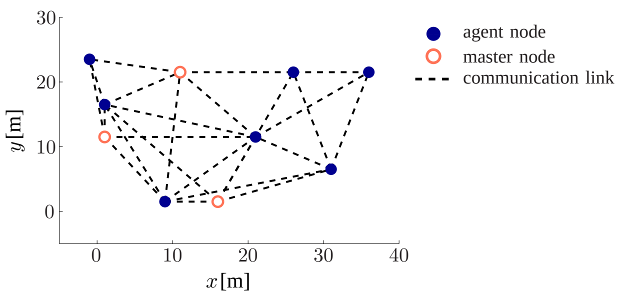

Fig. 1. Example of a sensor network with ANs and MNs.

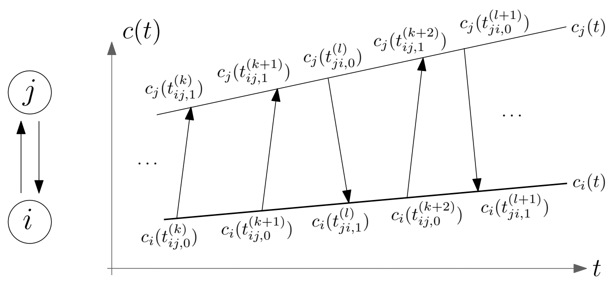

Fig. 2. Local clock functions $c_i(t)$ and $c_j(t)$, local time measurements (time stamps), and corresponding packet transmissions for nodes i and j.

(see Fig. 2). Node i transmits K_{ij} packets to node j, with the kth packet ($k \in \{1, \dots, K_{ij}\}$) leaving node i at time $t_{ij,0}^{(k)}$ and arriving at node j at measured time

$$t_{ij,1}^{(k)} = t_{ij,0}^{(k)} + \delta_{ij}^{(k)}, \quad \text{with } \delta_{ij}^{(k)} = \frac{d_{ij}}{v_0} + u_{ij}^{(k)}. \tag{2}$$

Here, $\delta_{ij}^{(k)}$ is the delay expressed in true time, $d_{ij} \triangleq \|\mathbf{x}_i - \mathbf{x}_j\|$ is the distance between nodes i and j, v_0 is the speed of light, and $u_{ij}^{(k)} \sim \mathcal{N}(0, \sigma_u^2)$ is Gaussian measurement noise that is independent across i, j, and k. The transmit and receive times are recorded in local time, resulting in the time stamps $c_i(t_{ij,0}^{(k)})$ and $c_j(t_{ij,1}^{(k)})$, respectively. It follows from (1) and (2) that $c_i(t_{ij,0}^{(k)})$ and $c_j(t_{ij,1}^{(k)})$ are related as

$$c_j(t_{ij,1}^{(k)}) \,=\, \psi_{i\to j}^{(k)}(\boldsymbol{\theta}_i, \boldsymbol{\theta}_j) + u_{ij}^{(k)} \alpha_j \,, \tag{3}$$

with

$$\psi_{i\to j}^{(k)}(\boldsymbol{\theta}_i, \boldsymbol{\theta}_j) \,\triangleq\, \frac{c_i(t_{ij,0}^{(k)}) - \beta_i}{\alpha_i} \alpha_j + \beta_j + \frac{d_{ij}}{v_0} \alpha_j \,. \tag{4}$$

Similarly, node j transmits K_{ji} packets to node i, resulting in the time stamps $c_j(t_{ji,0}^{(k)})$ and $c_i(t_{ji,1}^{(k)})$ ($k \in \{1, \dots, K_{ji}\}$). We require $K_{ij} + K_{ji} \geq 3$ (cf. Section IV). A relation between $c_j(t_{ji,0}^{(k)})$ and $c_i(t_{ji,1}^{(k)})$ is obtained by exchanging i and j in (3), (4). All time stamps are communicated to the respective other node. Thus, the aggregated measurement of nodes i and j is given by $\mathbf{c}_{ij} \triangleq [\mathbf{c}_{i\to j}^{\mathrm{T}} \; \mathbf{c}_{j\to i}^{\mathrm{T}}]^{\mathrm{T}}$, with $\mathbf{c}_{i\to j} \triangleq \big[c_j(t_{ij,1}^{(1)}) \cdots c_j(t_{ij,1}^{(K_{ij})})\big]^{\mathrm{T}}$ and $\mathbf{c}_{j\to i} \triangleq \big[c_i(t_{ji,1}^{(1)}) \cdots c_i(t_{ji,1}^{(K_{ji})})\big]^{\mathrm{T}}$. These measured time stamp vectors are complemented by the (recorded, not measured) transmit time stamp vectors $\tilde{\mathbf{c}}_{i\to j} \triangleq \big[c_i(t_{ij,0}^{(1)}) \cdots c_i(t_{ij,0}^{(K_{ij})})\big]^{\mathrm{T}}$ and $\tilde{\mathbf{c}}_{j\to i} \triangleq \big[c_j(t_{ji,0}^{(1)}) \cdots c_j(t_{ji,0}^{(K_{ji})})\big]^{\mathrm{T}}$.

B. Statistical Model

The problem to be solved is cooperative simultaneous estimation of the local parameters $\boldsymbol{\theta}_i$ of all ANs $i \in \mathcal{A}$ from all measured time stamps $\mathbf{c} \triangleq [\mathbf{c}_{ij}]_{(i,j)\in\mathcal{C}}$. Bayesian estimation relies on the posterior pdf of the $\boldsymbol{\theta}_i$, which in turn involves the likelihood functions $f(\mathbf{c}_{ij}|\boldsymbol{\theta}_i, \boldsymbol{\theta}_j)$ and the prior pdfs $f(\boldsymbol{\theta}_i)$.

The likelihood function of node pair $(i,j) \in \mathcal{C}$ follows from (3) and the statistical properties of the $u_{ij}^{(k)}$. We obtain

$$f(\mathbf{c}_{ij}|\boldsymbol{\theta}_i, \boldsymbol{\theta}_j) = G_{ij} \exp\!\left(-\frac{\|\mathbf{c}_{i\to j} - \boldsymbol{\psi}_{i\to j}\|^2}{2\alpha_j^2 \sigma_u^2} - \frac{\|\mathbf{c}_{j\to i} - \boldsymbol{\psi}_{j\to i}\|^2}{2\alpha_i^2 \sigma_u^2} \right),$$

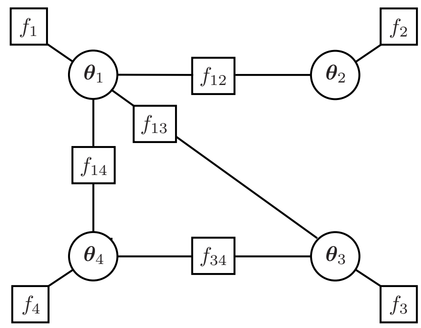

Fig. 3. Example factor graph of a network with node set $\mathcal{I} = \{1,2,3,4\}$. Variable nodes and factor nodes are depicted by circles and rectangles, respectively. The shorthands $f_i \triangleq f(\boldsymbol{\theta}_i)$ and $f_{ij} \triangleq f(\mathbf{c}_{ij}|\boldsymbol{\theta}_i, \boldsymbol{\theta}_j)$ are used.

where $G_{ij} \triangleq (2\pi\alpha_j^2\sigma_u^2)^{-K_{ij}/2}(2\pi\alpha_i^2\sigma_u^2)^{-K_{ji}/2}$, $\boldsymbol{\psi}_{i\to j} \triangleq \big[\psi_{i\to j}^{(k)}(\boldsymbol{\theta}_i, \boldsymbol{\theta}_j)\big]_{k=1}^{K_{ij}}$, and $\boldsymbol{\psi}_{j\to i} \triangleq \big[\psi_{j\to i}^{(k)}(\boldsymbol{\theta}_j, \boldsymbol{\theta}_i)\big]_{k=1}^{K_{ji}}$. Furthermore, since $\mathbf{c}_{ij}$ and $\mathbf{c}_{i'j'}$ are conditionally independent unless $(i,j) = (i',j')$, the global likelihood function is given by

$$f(\mathbf{c}|\boldsymbol{\theta}) \,=\, \prod_{\substack{(i,j)\in\mathcal{C} \\ i>j}} f(\mathbf{c}_{ij}|\boldsymbol{\theta}_i, \boldsymbol{\theta}_j)\,, \tag{5}$$

with the total parameter vector $\boldsymbol{\theta} \triangleq [\boldsymbol{\theta}_i]_{i\in\mathcal{I}}$.

For the ANs, the prior pdf of the clock skew α_i is $f(\alpha_i) = \mathcal{N}(\mu_{\alpha_i}, \sigma_{\alpha_i}^2)$, where $\mu_{\alpha_i} = 1$ and $\sigma_{\alpha_i}^2$ is typically given by the oscillator specification. The prior pdf of the phase offset, $f(\beta_i)$, is uniform on $[-b, b]$ (for some b) since no prior information about β_i is available. Similarly, the prior pdf $f(\mathbf{x}_i)$ is uniform on the entire localization area. For the MNs, we use $f(\boldsymbol{\theta}_i) = \delta(\boldsymbol{\theta}_i - \tilde{\boldsymbol{\theta}}_i)$, where $\tilde{\boldsymbol{\theta}}_i$ denotes the true local parameter vector of MN i and $\delta(\cdot)$ denotes the Dirac delta function. Finally, the local parameter vectors of all nodes are assumed *a priori* independent, and thus the joint prior pdf is

$$f(\boldsymbol{\theta}) = \prod_{i\in\mathcal{I}} f(\boldsymbol{\theta}_i)\,. \tag{6}$$

III. A Particle-based BP Algorithm

Using Bayes' rule and (5) and (6), the posterior pdf of the total parameter vector $\boldsymbol{\theta}$ can be factorized as

$$f(\boldsymbol{\theta}|\mathbf{c}) \,\propto\, f(\mathbf{c}|\boldsymbol{\theta}) f(\boldsymbol{\theta}) \,=\, \prod_{\substack{(i,j)\in\mathcal{C} \\ i>j}} f(\mathbf{c}_{ij}|\boldsymbol{\theta}_i, \boldsymbol{\theta}_j) \prod_{i'\in\mathcal{I}} f(\boldsymbol{\theta}_{i'})\,.$$

This factorization of $f(\boldsymbol{\theta}|\mathbf{c})$ can be expressed by a factor graph [12]; an example is shown in Fig. 3. We note that our factorization is "less detailed" than that used in [13], which implies that the factor graph contains fewer loops. More specifically, the factor graph has the same loop structure as the communication graph of the network, and hence is a tree (loopless) if the communication graph is a tree. By contrast, the factor graph corresponding to the factorization in [13] always contains multiple loops.

A. Message Passing Scheme

Bayesian estimation of the AN parameters $\boldsymbol{\theta}_i$, $i \in \mathcal{A}$ from $\mathbf{c}$ relies on the marginal posterior pdfs $f(\boldsymbol{\theta}_i|\mathbf{c}) = \int f(\boldsymbol{\theta}|\mathbf{c})\, d\boldsymbol{\theta}_{\sim i}$,

$i \in \mathcal{A}$ (here, $\boldsymbol{\theta}_{\sim i}$ denotes $\boldsymbol{\theta}$ with the subvector $\boldsymbol{\theta}_i$ removed). Based on the factor graph, approximations of the marginal posteriors, $b(\boldsymbol{\theta}_i) \approx f(\boldsymbol{\theta}_i|\mathbf{c})$, can be obtained by executing iterative BP message passing [12]. At message passing iteration $p \geq 1$, the "belief" $b^{(p)}(\boldsymbol{\theta}_i)$ is obtained as

$$b^{(p)}(\boldsymbol{\theta}_i) \propto f(\boldsymbol{\theta}_i) \prod_{j\in\mathcal{T}_i} m_{j\to i}^{(p)}(\boldsymbol{\theta}_i)\,, \tag{7}$$

with the messages

$$m_{j\to i}^{(p)}(\boldsymbol{\theta}_i) = \int f(\mathbf{c}_{ij}|\boldsymbol{\theta}_i,\boldsymbol{\theta}_j)\, n_{j\to i}^{(p-1)}(\boldsymbol{\theta}_j)\, d\boldsymbol{\theta}_j\,, \tag{8}$$

where

$$n_{j\to i}^{(p-1)}(\boldsymbol{\theta}_j) = f(\boldsymbol{\theta}_j) \prod_{i'\in\mathcal{T}_j\setminus\{i\}} m_{i'\to j}^{(p-1)}(\boldsymbol{\theta}_j)\,. \tag{9}$$

The "extrinsic" messages $n_{j\to i}^{(p-1)}(\boldsymbol{\theta}_j)$ were received from the neighboring sensors $j \in \mathcal{T}_i$ via packet transmissions. This message passing scheme is initialized by $n_{j\to i}^{(0)}(\boldsymbol{\theta}_j) = f(\boldsymbol{\theta}_j)$.

B. Particle-based Implementation

We propose a computationally feasible implementation of the BP algorithm (7)–(9) in which the messages are represented by particles (samples) and weights. As a difference from the original nonparametric BP algorithm introduced in [9] and used in the alternative CoSLAS algorithm in [13], our algorithm employs a novel scheme for particle-based message multiplication. The complexity of this scheme is only linear in the number of particles.

In the following, we describe the particle-based calculation of the belief $b^{(p)}(\boldsymbol{\theta}_i)$ at AN $i \in \mathcal{A}$ and message passing iteration p. By inserting (8) into (7), $b^{(p)}(\boldsymbol{\theta}_i)$ can be expressed as

$$b^{(p)}(\boldsymbol{\theta}_i) \propto \int b^{(p)}(\bar{\boldsymbol{\theta}}_i)\, d\bar{\boldsymbol{\theta}}_{\sim i}\,, \tag{10}$$

where $\bar{\boldsymbol{\theta}}_i \triangleq [\boldsymbol{\theta}_j]_{j\in\{i\}\cup\mathcal{T}_i}$, $\bar{\boldsymbol{\theta}}_{\sim i}$ denotes $\bar{\boldsymbol{\theta}}_i$ with the subvector $\boldsymbol{\theta}_i$ removed, and

$$b^{(p)}(\bar{\boldsymbol{\theta}}_i) \triangleq f(\boldsymbol{\theta}_i) \prod_{j\in\mathcal{T}_i} f(\mathbf{c}_{ij}|\boldsymbol{\theta}_i,\boldsymbol{\theta}_j)\, n_{j\to i}^{(p-1)}(\boldsymbol{\theta}_j)\,. \tag{11}$$

Therefore, a particle representation (PR) $\big\{\big(\boldsymbol{\theta}_i^{(l)}, w_i^{(l)}\big)\big\}_{l=1}^{L}$ of $b^{(p)}(\boldsymbol{\theta}_i)$ can be obtained by first calculating a PR $\big\{\big(\bar{\boldsymbol{\theta}}_i^{(l)}, w_i^{(l)}\big)\big\}_{l=1}^{L}$ of $b^{(p)}(\bar{\boldsymbol{\theta}}_i)$, as discussed presently, and then simulating the marginalization in (10) by extracting $\boldsymbol{\theta}_i^{(l)}$ from $\bar{\boldsymbol{\theta}}_i^{(l)}$, i.e., discarding all entries corresponding to $\bar{\boldsymbol{\theta}}_{\sim i}$ [15]. From the PR $\big\{\big(\boldsymbol{\theta}_i^{(l)}, w_i^{(l)}\big)\big\}_{l=1}^{L}$, an approximation of the minimum mean-square error estimate of $\boldsymbol{\theta}_i$ can finally be obtained as

$$\hat{\boldsymbol{\theta}}_i = \sum_{l=1}^{L} w_i^{(l)} \boldsymbol{\theta}_i^{(l)}.$$

To calculate the PR $\big\{\big(\bar{\boldsymbol{\theta}}_i^{(l)}, w_i^{(l)}\big)\big\}_{l=1}^{L}$, we employ importance sampling using the proposal pdf

$$q^{(p)}(\bar{\boldsymbol{\theta}}_i) \propto q^{(p)}(\boldsymbol{\theta}_i) \prod_{j\in\mathcal{T}_i} n_{j\to i}^{(p-1)}(\boldsymbol{\theta}_j)\,. \tag{12}$$

Here, $q^{(p)}(\boldsymbol{\theta}_i)$ is a suitable proposal pdf for $\boldsymbol{\theta}_i$ whose choice will be discussed in Section IV. To obtain particles representing $q^{(p)}(\bar{\boldsymbol{\theta}}_i)$, we first draw particles $\big\{\boldsymbol{\theta}_i^{(l)}\big\}_{l=1}^{L}$ from $q^{(p)}(\boldsymbol{\theta}_i)$. (These particles are directly used for the PR $\big\{\big(\boldsymbol{\theta}_i^{(l)}, w_i^{(l)}\big)\big\}_{l=1}^{L}$ of $b^{(p)}(\boldsymbol{\theta}_i)$; the steps described in what follows serve only to calculate the associated weights $w_i^{(l)}$.) In addition, particles $\big\{\boldsymbol{\theta}_j^{(l)}\big\}_{l=1}^{L}$ representing $n_{j\to i}^{(p-1)}(\boldsymbol{\theta}_j)$ were received from the neighboring sensors $j \in \mathcal{T}_i$. Then, based on (12), we form $\bar{\boldsymbol{\theta}}_i^{(l)}$ by stacking $\boldsymbol{\theta}_i^{(l)}$ and the $\boldsymbol{\theta}_j^{(l)}$, $j \in \mathcal{T}_i$ in the order used in the definition of $\bar{\boldsymbol{\theta}}_i$. Finally, following the importance sampling principle, we obtain weights $w_i^{(l)}$ by evaluating $w^{(p)}(\bar{\boldsymbol{\theta}}_i) \triangleq b^{(p)}(\bar{\boldsymbol{\theta}}_i)/q^{(p)}(\bar{\boldsymbol{\theta}}_i)$ at the particles $\bar{\boldsymbol{\theta}}_i^{(l)}$ and normalizing, i.e., $w_i^{(l)} = w^{(p)}(\bar{\boldsymbol{\theta}}_i^{(l)})/W_i$ with $W_i = \sum_{l=1}^{L} w^{(p)}(\bar{\boldsymbol{\theta}}_i^{(l)})$. We note that using (11) and (12), $w^{(p)}(\bar{\boldsymbol{\theta}}_i)$ is obtained as

$$w^{(p)}(\bar{\boldsymbol{\theta}}_i) = \frac{f(\boldsymbol{\theta}_i)\prod_{j\in\mathcal{T}_i} f(\mathbf{c}_{ij}|\boldsymbol{\theta}_i,\boldsymbol{\theta}_j)}{q^{(p)}(\boldsymbol{\theta}_i)}\,.$$

In addition to a PR of the belief $b^{(p)}(\boldsymbol{\theta}_i)$, PRs of the extrinsic messages $n_{i\to j}^{(p)}(\boldsymbol{\theta}_i)$, $j \in \mathcal{T}_i$ have to be calculated at node $i \in \mathcal{A}$. These PRs are transmitted to all nodes $j \in \mathcal{T}_i$, where they are used in the calculation of a PR of $b^{(p+1)}(\boldsymbol{\theta}_j)$. A PR of $n_{i\to j}^{(p)}(\boldsymbol{\theta}_i)$, $j \in \mathcal{T}_i$ (cf. (9)) can be obtained in a similar manner as for $b^{(p)}(\boldsymbol{\theta}_i)$, due to the structural analogy of (9) to (7). However, here we perform an additional resampling [15] to obtain equally weighted particles representing $n_{i\to j}^{(p)}(\boldsymbol{\theta}_i)$.

This particle-based BP implementation differs from the conventional nonparametric BP scheme in [9] and [13] in that importance sampling is performed for a higher-dimensional pdf, namely, the pdf of the "stacked state" $\bar{\boldsymbol{\theta}}_i$. Therefore, the number of particles L has typically to be chosen higher than in nonparametric BP. On the other hand, the complexity of the operations performed at node $i \in \mathcal{A}$ scales as $\mathcal{O}(L|\mathcal{T}_i|)$, i.e., only linearly in L, whereas the complexity of nonparametric BP is quadratic in L [16]. For this reason, the complexity of our scheme tends to be lower than that of nonparametric BP.

At each message passing iteration p, a set of $4L$ real values has to be transmitted from each node $i \in \mathcal{I}$ to each neighbor $j \in \mathcal{T}_i$ (one set for each extrinsic message $n_{i\to j}^{(p)}(\boldsymbol{\theta}_i)$). Thus, the communication requirements increase linearly with L, and they are typically higher than those of nonparametric BP. However, this disadvantage can be avoided by using parametric representations of the extrinsic messages for communication [14]. An example will be considered in Section V.

IV. Calculation of the Proposal Distribution

It remains to discuss the calculation of the proposal pdf $q^{(p)}(\boldsymbol{\theta}_i)$ used in (12). In particle-based BP, frequently one of the incoming messages $m_{j\to i}^{(p)}(\boldsymbol{\theta}_i)$, $j \in \mathcal{T}_i$ in (8) is used as proposal pdf [9], [16]. Therefore, we next consider the calculation of a PR of $m_{j\to i}^{(p)}(\boldsymbol{\theta}_i) = \int f(\mathbf{c}_{ij}|\boldsymbol{\theta}_i,\boldsymbol{\theta}_j)\, n_{j\to i}^{(p-1)}(\boldsymbol{\theta}_j)\, d\boldsymbol{\theta}_j$ from a PR $\big\{\big(\boldsymbol{\theta}_j^{(l)}, w^{(l)}\big)\big\}_{l=1}^{L}$ of $n_{j\to i}^{(p-1)}(\boldsymbol{\theta}_j)$, based on the "message filtering" scheme proposed in [9] and [16]. (Note that $\mathbf{c}_{ij}$ is measured and thus considered fixed.)

Suppose for the moment that the local likelihood function $f(\mathbf{c}_{ij}|\boldsymbol{\theta}_i,\boldsymbol{\theta}_j)$ is consistent with some "$\boldsymbol{\theta}_j \to \boldsymbol{\theta}_i$ relation"

$\boldsymbol{\theta}_i = r(\mathbf{c}_{ij}, \boldsymbol{\theta}_j, \mathbf{v}_{ij})$, with a "transition function" $r(\mathbf{c}_{ij}, \boldsymbol{\theta}_j, \mathbf{v}_{ij})$ and a random vector $\mathbf{v}_{ij}$ that is independent of $\boldsymbol{\theta}_i$ and $\boldsymbol{\theta}_j$ and whose pdf $f(\mathbf{v}_{ij})$ can be sampled. Then, a PR $\big\{\big(\boldsymbol{\theta}_i^{(l)}, \boldsymbol{\theta}_j^{(l)}, w^{(l)}\big)\big\}_{l=1}^{L}$ of $f(\mathbf{c}_{ij}|\boldsymbol{\theta}_i, \boldsymbol{\theta}_j)\, n_{j\to i}^{(p-1)}(\boldsymbol{\theta}_j)$ (with $\boldsymbol{\theta}_j^{(l)}$ and $w^{(l)}$ as before) can be established by first drawing L particles $\big\{\mathbf{v}_{ij}^{(l)}\big\}_{l=1}^{L}$ from $f(\mathbf{v}_{ij})$ and then evaluating $r(\mathbf{c}_{ij}, \boldsymbol{\theta}_j, \mathbf{v}_{ij})$ at $\big\{\big(\boldsymbol{\theta}_j^{(l)}, \mathbf{v}_{ij}^{(l)}\big)\big\}_{l=1}^{L}$, i.e., $\boldsymbol{\theta}_i^{(l)} = r(\mathbf{c}_{ij}, \boldsymbol{\theta}_j^{(l)}, \mathbf{v}_{ij}^{(l)})$, $l \in \{1, \ldots, L\}$. Furthermore, a PR of $m_{j\to i}^{(p)}(\boldsymbol{\theta}_i) = \int f(\mathbf{c}_{ij}|\boldsymbol{\theta}_i, \boldsymbol{\theta}_j) \times n_{j\to i}^{(p-1)}(\boldsymbol{\theta}_j)\, d\boldsymbol{\theta}_j$ is then given by $\big\{\big(\boldsymbol{\theta}_i^{(l)}, w^{(l)}\big)\big\}_{l=1}^{L}$.

However, this message filtering scheme cannot be used in a straightforward manner because for our local likelihood function $f(\mathbf{c}_{ij}|\boldsymbol{\theta}_i, \boldsymbol{\theta}_j)$, a transition function $r(\mathbf{c}_{ij}, \boldsymbol{\theta}_j, \mathbf{v}_{ij})$ is not available in general. Therefore, we introduce new "pseudomeasurements" $\bar{\mathbf{c}}_{ij}$ and a corresponding modified local likelihood function $f(\bar{\mathbf{c}}_{ij}|\boldsymbol{\theta}_i, \boldsymbol{\theta}_j)$ for which a $\boldsymbol{\theta}_j \to \boldsymbol{\theta}_i$ relation $\boldsymbol{\theta}_i = r(\bar{\mathbf{c}}_{ij}, \boldsymbol{\theta}_j, \mathbf{v}_{ij})$ can be established. We define the pseudomeasurements as $\bar{\mathbf{c}}_{ij} \triangleq \big[\bar{c}_{ij}^{(1)}\ \bar{c}_{ij}^{(2)}\ \bar{c}_{ij}^{(3)}\big]^{\mathrm{T}}$, where the $\bar{c}_{ij}^{(\nu)}$ are the following averages of the available measurements $\mathbf{c}_{ij}$:

$$\bar{c}_{ij}^{(1)} \triangleq \frac{1}{\tilde{K}_{ji}} \sum_{k=1}^{\tilde{K}_{ji}} c_j(t_{ji,1}^{(k)})$$

$$\bar{c}_{ij}^{(2)} \triangleq \frac{1}{K_{ji} - \tilde{K}_{ji}} \sum_{k=\tilde{K}_{ji}+1}^{K_{ji}} c_j(t_{ji,1}^{(k)})$$

$$\bar{c}_{ij}^{(3)} \triangleq \frac{1}{K_{ij}} \sum_{k=1}^{K_{ij}} c_i(t_{ij,1}^{(k)})\,,$$

with $\tilde{K}_{ji} = \lceil K_{ji}/2 \rceil$. (There is some freedom in defining the components $\bar{c}_{ij}^{(\nu)}$; for example, an alternative definition is obtained by interchanging i and j in the above expressions.) We furthermore define a transformed parameter $\tilde{\boldsymbol{\theta}}_i \triangleq \big[\tilde{\theta}_i^{(1)}\ \tilde{\theta}_i^{(2)}\ \tilde{\theta}_i^{(3)}\big]^{\mathrm{T}}$, with

$$\tilde{\theta}_i^{(1)} \triangleq \frac{\beta_i}{\alpha_i}\,, \quad \tilde{\theta}_i^{(2)} \triangleq \frac{1}{\alpha_i}\,, \quad \tilde{\theta}_i^{(3)} \triangleq d_{ij}\,. \tag{13}$$

Using (3) and (4), one can then derive the following linear equation:

$$\mathbf{A}_{ij} \tilde{\boldsymbol{\theta}}_i = \mathbf{b}_{ij}\,, \tag{14}$$

with

$$\mathbf{A}_{ij} = \begin{bmatrix} \alpha_j & -\frac{\alpha_j}{\tilde{K}_{ji}} \sum_{k=1}^{\tilde{K}_{ji}} c_j(t_{ji,0}^{(k)}) & -\alpha_j/v_0 \\ \alpha_j & -\frac{\alpha_j}{K_{ji}-\tilde{K}_{ji}} \sum_{k=\tilde{K}_{ji}+1}^{K_{ji}} c_j(t_{ji,0}^{(k)}) & -\alpha_j/v_0 \\ -1 & \bar{c}_{ij}^{(3)} & -1/v_0 \end{bmatrix}$$

$$\mathbf{b}_{ij} = \begin{bmatrix} \beta_j + \frac{\alpha_j}{\tilde{K}_{ji}} \sum_{k=1}^{\tilde{K}_{ji}} u_{ji}^{(k)} - \bar{c}_{ij}^{(1)} \\ \beta_j + \frac{\alpha_j}{K_{ji}-\tilde{K}_{ji}} \sum_{k=\tilde{K}_{ji}+1}^{K_{ji}} u_{ji}^{(k)} - \bar{c}_{ij}^{(2)} \\ \frac{1}{\alpha_j K_{ij}} \sum_{k=1}^{K_{ij}} c_i(t_{ij,0}^{(k)}) - \frac{\beta_j}{\alpha_j} + \frac{1}{K_{ij}} \sum_{k=1}^{K_{ij}} u_{ij}^{(k)} \end{bmatrix}.$$

Note that $\mathbf{A}_{ij}$ and $\mathbf{b}_{ij}$ depend only on $\boldsymbol{\theta}_j$ (more specifically, on α_j and β_j), the pseudomeasurements $\bar{\mathbf{c}}_{ij}$, and the measurement noise vector $\mathbf{u}_{ij} \triangleq \big[u_{ij}^{(1)} \cdots u_{ij}^{(K_{ij})}\ u_{ji}^{(1)} \cdots u_{ji}^{(K_{ji})}\big]^{\mathrm{T}}$ (and, also, on the recorded time stamps $c_i(t_{ij,0}^{(k)})$ and $c_j(t_{ji,0}^{(k)})$); they do not depend on $\boldsymbol{\theta}_i$ or $\tilde{\boldsymbol{\theta}}_i$. Solving (14) yields $\tilde{\boldsymbol{\theta}}_i = \mathbf{A}_{ij}^{-1} \mathbf{b}_{ij}$, which can be written as

$$\tilde{\boldsymbol{\theta}}_i = h(\bar{\mathbf{c}}_{ij}, \boldsymbol{\theta}_j, \mathbf{u}_{ij})\,. \tag{15}$$

Furthermore, using (13), it is seen that $\boldsymbol{\theta}_i$ is related to $\tilde{\boldsymbol{\theta}}_i$ and $\boldsymbol{\theta}_j$ as $\boldsymbol{\theta}_i = \big[x_j + \tilde{\theta}_i^{(3)} \cos(\phi_{ij})\ \ y_j + \tilde{\theta}_i^{(3)} \sin(\phi_{ij})\ \ 1/\tilde{\theta}_i^{(2)}\ \ \tilde{\theta}_i^{(1)}/\tilde{\theta}_i^{(2)}\big]^{\mathrm{T}}$, where ϕ_{ij} is the (unknown) azimuth angle of the vector $\mathbf{x}_j - \mathbf{x}_i$. We can thus write

$$\boldsymbol{\theta}_i = g(\tilde{\boldsymbol{\theta}}_i, \boldsymbol{\theta}_j, \phi_{ij})\,. \tag{16}$$

Inserting (15) into (16), we finally obtain the desired $\boldsymbol{\theta}_j \to \boldsymbol{\theta}_i$ relation as

$$\boldsymbol{\theta}_i = r(\bar{\mathbf{c}}_{ij}, \boldsymbol{\theta}_j, \mathbf{v}_{ij}) \triangleq g(h(\bar{\mathbf{c}}_{ij}, \boldsymbol{\theta}_j, \mathbf{u}_{ij}), \boldsymbol{\theta}_j, \phi_{ij})\,, \tag{17}$$

with $\mathbf{v}_{ij} \triangleq \big[\mathbf{u}_{ij}^{\mathrm{T}}\ \ \phi_{ij}\big]^{\mathrm{T}}$. This relation (and transition function r) is consistent with the modified local likelihood function $f(\bar{\mathbf{c}}_{ij}|\boldsymbol{\theta}_i, \boldsymbol{\theta}_j)$.

We now use the "pseudomessage" $\bar{m}_{j_0\to i}^{(p)}(\boldsymbol{\theta}_i) \triangleq \int f(\bar{\mathbf{c}}_{ij_0}|\boldsymbol{\theta}_i, \boldsymbol{\theta}_{j_0})\, n_{j_0\to i}^{(p-1)}(\boldsymbol{\theta}_{j_0})\, d\boldsymbol{\theta}_{j_0}$ as proposal pdf $q^{(p)}(\boldsymbol{\theta}_i)$ (up to a normalization). Here, j_0 is randomly chosen from the set of neighboring MNs, $\mathcal{M}_i \triangleq \mathcal{M} \cap \mathcal{T}_i$, or from the set of all neighbors, $\mathcal{T}_i$, if $\mathcal{M}_i$ is empty. Our numerical analysis suggested that $\bar{m}_{j_0\to i}^{(p)}(\boldsymbol{\theta}_i)$ is a good approximation of $m_{j_0\to i}^{(p)}(\boldsymbol{\theta}_i)$. Using the particles $\big\{\boldsymbol{\theta}_{j_0}^{(l)}\big\}_{l=1}^{L}$ representing $n_{j_0\to i}^{(p-1)}(\boldsymbol{\theta}_{j_0})$, which are available at AN i, we can perform message filtering for $\bar{m}_{j_0\to i}^{(p)}(\boldsymbol{\theta}_i) = \int f(\bar{\mathbf{c}}_{ij_0}|\boldsymbol{\theta}_i, \boldsymbol{\theta}_{j_0})\, n_{j_0\to i}^{(p-1)}(\boldsymbol{\theta}_{j_0})\, d\boldsymbol{\theta}_{j_0}$ by invoking (17), i.e., calculating

$$\boldsymbol{\theta}_i^{(l)} = r\big(\bar{\mathbf{c}}_{ij_0}, \boldsymbol{\theta}_{j_0}^{(l)}, \mathbf{v}_{ij_0}^{(l)}\big)\,, \quad l \in \{1, \ldots, L\}\,,$$

with $\mathbf{v}_{ij_0}^{(l)} = \big[\mathbf{u}_{ij_0}^{(l)\mathrm{T}}\ \ \phi_{ij_0}^{(l)}\big]^{\mathrm{T}}$. Here, the particles $\big\{\mathbf{u}_{ij_0}^{(l)}\big\}_{l=1}^{L}$ are drawn from $\mathcal{N}(\mathbf{0}, \sigma_u^2 \mathbf{I})$ and the particles $\big\{\phi_{ij_0}^{(l)}\big\}_{l=1}^{L}$ are drawn uniformly on $[0, 2\pi)$.

V. Simulation Results

We simulated a network consisting of seven ANs and three MNs. The node locations and communication graph are shown in Fig. 1. The numbers of time stamp transmissions/measurements were $K_{ij} = K_{ji} = 50$, and the measurement noise variance was $\sigma_u^2 = 5 \times 10^{-15}\,\mathrm{s}^2$. The clock parameters α_i and β_i were randomly drawn from, respectively, a Gaussian distribution with mean 1 and standard deviation 10^{-4} (= 100 ppm) and a uniform distribution on the interval $[-1\mathrm{s}, 1\mathrm{s}]$. The location prior used for algorithm simulation was uniform on $[-100\,\mathrm{m}, 100\,\mathrm{m}] \times [-100\,\mathrm{m}, 100\,\mathrm{m}]$.

We compare the proposed particle-based BP algorithm for CoSLAS (abbreviated as "CoSLAS-PBP") with the hybrid BP algorithm for CoSLAS proposed in [13] ("CoSLAS-HBP") and a state-of-the-art algorithm that separately performs synchronization by means of the method described in [11] ("Sync-BP") and localization by means of nonparametric (particle-based) BP as described in [9] ("Loc-PBP"). Loc-PBP uses the clock estimates provided by Sync-BP only after the fourth message passing iteration, i.e., after sufficient convergence of Sync-BP. We also simulated a variant of CoSLAS-PBP ("CoSLAS-PBPG") in which the extrinsic messages $n_{j\to i}^{(p-1)}(\boldsymbol{\theta}_j)$ are approximated by a mixture of two

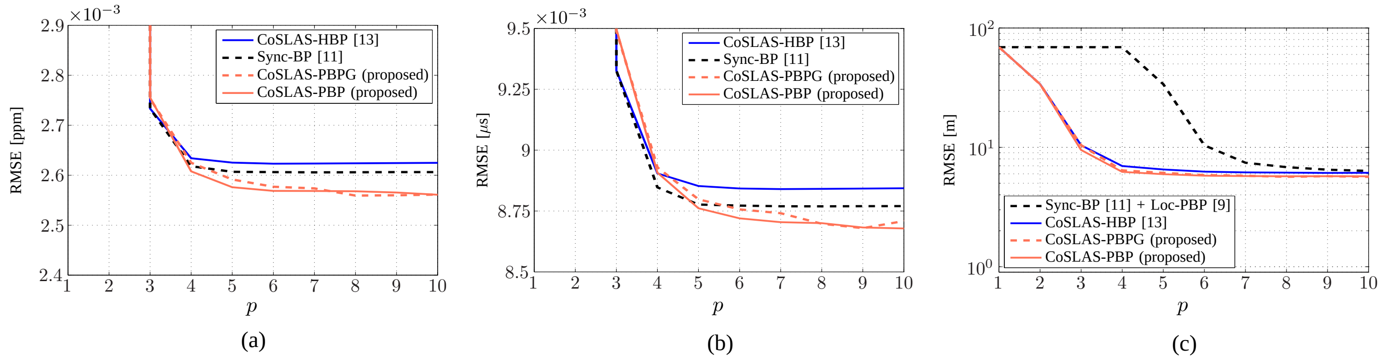

Fig. 4. Average RMSE of (a) clock skew, (b) clock phase, and (c) location versus message passing iteration index p.

equally weighted Gaussians before being transmitted to neighboring nodes (as proposed in [14]). Here, each node transmits only the means and covariance matrices of the two Gaussian components, which corresponds to 28 (instead of $4L$) real values per message passing iteration. The number of samples, L, was 50000 for CoSLAS-PBP and CoSLAS-PBPG and 1000 for CoSLAS-HBP and Loc-PBP. We emphasize that, in spite of the significantly higher number of particles, CoSLAS-PBP and CoSLAS-PBPG are still less complex than both CoSLAS-HBP and the state-of-the-art algorithm (Sync-BP + Loc-PBP).

In Fig. 4, we show the average (i.e., averaged over all nodes and 1000 simulation runs) root-mean-square-errors (RMSEs) of clock skew estimation, clock phase estimation, and location estimation. It can be seen that in the simulated scenario, the proposed CoSLAS-PBP and CoSLAS-PBPG algorithms outperform CoSLAS-HBP and the state-of-the-art algorithm. This can be explained by the fact that approximations of the likelihood function as in Sync-BP and CoSLAS-HBP are avoided and the factor graph has fewer loops (compared to CoSLAS-HBP). Note, however, that a high number of particles is needed, which implies high memory requirements. It is furthermore seen that CoSLAS-PBPG performs almost as well as CoSLAS-PBP, in spite of the dramatically reduced communication requirements. Finally, Fig. 4(c) shows that, with respect to the localization RMSE, CoSLAS-PBP, CoSLAS-PBPG, and CoSLAS-HBP converge significantly faster than the state-of-the-art algorithm.

VI. Conclusion

We presented a belief propagation algorithm for distributed *cooperative simultaneous localization and synchronization* (CoSLAS) in decentralized sensor networks. This algorithm jointly estimates the locations and clock parameters of the network nodes, thereby leveraging the strong interdependency of localization and synchronization within a coherent message passing scheme. The algorithm is fully decentralized, using only in-network processing and time measurements and communications only between neighboring nodes. We proposed a particle-based implementation that differs from conventional nonparametric belief propagation in that it employs a novel scheme for message multiplication. In many scenarios, this scheme results in a reduction of computational complexity compared to other particle-based CoSLAS and localization algorithms. Simulation results demonstrated that the proposed algorithm can outperform a hybrid (parametric and particle-based) CoSLAS algorithm and a reference method that separately performs synchronization and localization.

References

[1] H. Wymeersch, J. Lien, and M. Z. Win, "Cooperative localization in wireless networks," *Proc. IEEE*, vol. 97, pp. 427–450, Feb. 2009.

[2] O. Simeone, U. Spagnolini, Y. Bar-Ness, and S. H. Strogatz, "Distributed synchronization in wireless networks," *IEEE Signal Process. Mag.*, vol. 25, pp. 81–97, Jan. 2008.

[3] N. Patwari, J. N. Ash, S. Kyperountas, A. O. Hero III, R. L. Moses, and N. S. Correal, "Locating the nodes: Cooperative localization in wireless sensor networks," *IEEE Signal Process. Mag.*, vol. 22, pp. 54–69, Jul. 2005.

[4] D. Benoît, J.-B. Pierrot, and C. Abou-Rjeily, "Joint distributed synchronization and positioning in UWB ad hoc networks using TOA," *IEEE Trans. Microw. Theory Techn.*, vol. 54, pp. 1896–1911, Apr. 2006.

[5] J. Zheng and Y.-C. Wu, "Joint time synchronization and localization of an unknown node in wireless sensor networks," *IEEE Trans. Signal Process.*, vol. 58, pp. 1309–1320, Mar. 2010.

[6] S. Zhu and Z. Ding, "Joint synchronization and localization using TOAs: A linearization based WLS solution," *IEEE J. Sel. Areas Commun.*, vol. 28, pp. 1017–1025, Aug. 2010.

[7] S. P. Chepuri, G. Leus, and A.-J. van der Veen, "Joint localization and clock synchronization for wireless sensor networks," in *Proc. Asilomar Conf. Sig., Syst., Comput.*, Pacific Grove, CA, pp. 1432–1436, Nov. 2012.

[8] M. Sun and L. Yang, "On the joint time synchronization and source localization using TOA measurements," *Int. J. Dist. Sensor Netw.*, vol. 2013, Jan. 2013.

[9] A. T. Ihler, J. W. Fisher, R. L. Moses, and A. S. Willsky, "Nonparametric belief propagation for self-localization of sensor networks," *IEEE J. Sel. Areas Commun.*, vol. 23, pp. 809–819, Apr. 2005.

[10] M. Leng and Y.-C. Wu, "Distributed clock synchronization for wireless sensor networks using belief propagation," *IEEE Trans. Signal Process.*, vol. 59, pp. 5404–5414, Nov. 2011.

[11] B. Etzlinger, H. Wymeersch, and A. Springer, "Cooperative synchronization in wireless networks." *IEEE Trans. Signal Process.*, 2014, submitted. arXiv:1304.8029v2[cs.DC].

[12] F. Kschischang, B. Frey, and H.-A. Loeliger, "Factor graphs and the sum-product algorithm," *IEEE Trans. Inf. Theory*, vol. 47, pp. 498–519, Feb. 2001.

[13] B. Etzlinger, F. Meyer, A. Springer, F. Hlawatsch, and H. Wymeersch, "Cooperative simultaneous localization and synchronization: A distributed hybrid message passing algorithm," in *Proc. Asilomar Conf. Sig., Syst., Comput.*, Pacific Grove, CA, Nov. 2013.

[14] V. Savic and S. Zazo, "Reducing communication overhead for cooperative localization using nonparametric belief propagation," *IEEE Commun. Letters*, vol. 1, no. 4, pp. 308–311, 2012.

[15] A. Doucet, N. de Freitas, and N. Gordon, *Sequential Monte Carlo Methods in Practice*. New York, NY: Springer, 2001.

[16] J. Lien, J. Ferner, W. Srichavengsup, H. Wymeersch, and M. Z. Win, "A comparison of parametric and sample-based message representation in cooperative localization." *Int. J. Navig. Observ.*, 2012.